



HAL
open science

Ab initio study of electronic and crystal structure of $\text{Mo}_3\text{Sb}_{7-x}\text{Te}_x$ from KKR-CPA calculations and neutron diffraction measurements

Christophe Candolfi, Bertrand Lenoir, Anne Dauscher, Janusz Tobola, Simon Clarke, Ron Smith

► **To cite this version:**

Christophe Candolfi, Bertrand Lenoir, Anne Dauscher, Janusz Tobola, Simon Clarke, et al.. Ab initio study of electronic and crystal structure of $\text{Mo}_3\text{Sb}_{7-x}\text{Te}_x$ from KKR-CPA calculations and neutron diffraction measurements. *Chemistry of Materials*, 2008, 20 (20), pp.6556-6561. 10.1021/cm801560n . hal-03998425

HAL Id: hal-03998425

<https://hal.science/hal-03998425>

Submitted on 21 Feb 2023

HAL is a multi-disciplinary open access archive for the deposit and dissemination of scientific research documents, whether they are published or not. The documents may come from teaching and research institutions in France or abroad, or from public or private research centers.

L'archive ouverte pluridisciplinaire **HAL**, est destinée au dépôt et à la diffusion de documents scientifiques de niveau recherche, publiés ou non, émanant des établissements d'enseignement et de recherche français ou étrangers, des laboratoires publics ou privés.

***Ab initio* study of electronic and crystal structure of $\text{Mo}_3\text{Sb}_{7-x}\text{Te}_x$
from KKR-CPA calculations and neutron diffraction measurements**

Christophe Candolfi^{1*}, Bertrand Lenoir¹, Anne Dauscher¹, Janusz Tobola², Simon J.
Clarke³ and Ron I. Smith⁴

¹*Laboratoire de Physique des Matériaux, UMR 7556, Ecole Nationale Supérieure des
Mines de Nancy, Parc de Saurupt, 54042 Nancy cedex, France*

²*Faculty of Physics and Applied Computer Science, AGH University of Science and
Technology, 30-059 Krakow, Poland*

³*Inorganic Chemistry Laboratory, Department of Chemistry, University of Oxford, South
Parks Road, Oxford OX1 3 QR, UK*

⁴*ISIS Facility, Rutherford Appleton Laboratory, Chilton, Didcot, Oxon OX11 0QX, United
Kingdom*

* Corresponding author: candolfi@mines.inpl-nancy.fr

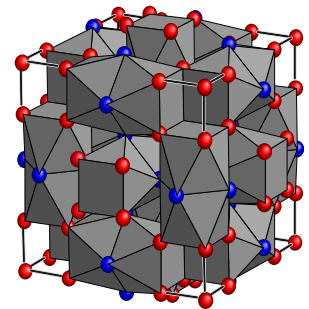
Keywords: band structure, neutron diffraction

Christophe Candolfi*, Bertrand Lenoir,
Anne Dauscher, Janusz Tobola, Simon J.
Clarke and Ron I. Smith

Chem. Mater.

Ab initio study of electronic and crystal
structure of $\text{Mo}_3\text{Sb}_{7-x}\text{Te}_x$ from KKR-CPA
calculations and neutron diffraction
measurements

Substitution of Sb by Te atoms in the Mo_3Sb_7
crystalline structure gives rise to a tellurium's
site preference that can be experimentally
demonstrated by neutron diffraction and
theoretically explained using band structure
calculations.



Abstract

Band structure calculations based on the KKR-CPA method have been undertaken on the $\text{Mo}_3\text{Sb}_{7-x}\text{Te}_x$ and $\text{Re}_3\text{As}_{7-x}\text{Ge}_x$ systems as well as neutron diffraction analysis on the polycrystalline Mo_3Sb_7 and $\text{Mo}_3\text{Sb}_{5.4}\text{Te}_{1.6}$ compounds. Both results strongly suggest that the Te atoms are only located on the $12d$ crystallographic site while the Ge atoms are located on the $16f$ site as previously experimentally underlined from neutron diffraction study. From an electronic point of view, this site preference in the $\text{Mo}_3\text{Sb}_{7-x}\text{Te}_x$ samples is well supported by total energy estimation and is presumably related to the reduction of the overall valence p -states of Te with respect to those of the $12d$ Sb site.

I. Introduction

Huge efforts have been made in the last decade to identify new thermoelectric materials for refrigeration and power generation applications.¹⁻⁵ To be an efficient converter, a thermoelectric material should exhibit a high dimensionless figure of merit, ZT , expressed as⁶

$$ZT = \frac{\alpha^2}{\rho\lambda} T$$

where α is the Seebeck coefficient or thermoelectric power, ρ the electrical resistivity, λ the total thermal conductivity composed of two terms: the lattice thermal conductivity λ_L and the carrier thermal conductivity λ_e , and T the absolute temperature. This equation clearly shows how tough the task is as a good candidate must conduct electricity like a crystal and impedes phonon transport e.g. having a glass-like behaviour.⁷ To achieve low thermal conductivity values, complex crystalline structures or compounds with weakly bounded atoms in oversized cages have been extensively studied.^{1,2,8-12} The former should bring low lattice thermal

conductivity values via strong disorder and mass fluctuations while the latter can rattle about their equilibrium position in their cages, disrupting harmonic modes of the parent atoms. The challenge then lies in maintaining low electrical resistivity. That is why narrow band gap semiconductors and small band overlapped semimetals stand for the best candidates.

Recently, it was shown that some intermetallic compounds based on M_3X_7 and crystallizing in the Ir_3Ge_7 -type structure can exhibit exotic phenomena at low temperature¹³⁻¹⁵ while they can be promising materials for power generation at high temperature.^{16,17} In the M_3X_7 structure, M is preferentially 4d and 5d transition metals while X can be either the triels Ga and In, the tetrels Ge and Sn or the pentels As and Sb. The crystal structure of the binary compound M_3X_7 (space group $Im\bar{3}m$, No. 229) is body-centred cubic and consists of an ensemble of two condensed antiprisms, sharing a square face formed by metalloid atoms (Figure 1a). The M atoms sit at the centre of these fundamental building blocks. The rotation angle between square faces is 45° whatever the compound is, resulting in two inequivalent sites for X atoms. The first one situated at the shared square face denotes the X1 (12d) positions, while the X atoms defining the opposite square faces correspond to the second site (16f), called X2. These units are joined together to a framework by sharing common edges of the terminal square faces and determine the empty cube surrounded by 8 X2 atoms as shown in Figure 1b. The centre of this cavity represents the site 2a (0, 0, 0). The size of the cavity is governed by only one variable, i.e. the x parameter of the site 16f (x, x, x), positioning the X2 atoms. Finally, the cubic unit cell of the M_3X_7 compound assembles the aforementioned blocks in such a way that the centers of the empty cubes are placed at the origin of the cell (Figure 1c).

First theoretical studies performed by Häussermann et al.¹⁸ shed some light on this family by suggesting that binary compounds exhibiting strong d - p interactions should be semiconducting when the number of valence electrons equals 55 per M_3X_7 formula unit (i.e.

VEC = 55). Later on, these assumptions were theoretically confirmed from LMTO calculations in both the $\text{Mo}_3\text{Sb}_{7-x}\text{Te}_x$ and $\text{Re}_3\text{As}_{7-x}\text{Ge}_x$ systems where the semiconducting state was predicted for $x = 2$ and $x = 1$ respectively.^{15,19} If these studies shown well that the former compound should display a p-type behaviour while the latter should exhibit n-type character, no detailed analysis has been made on the chemical disorder present in the crystalline structure. Since the transport properties are highly dependent on the band structure near the Fermi level, it is of prime importance from a fundamental point of view but also for experimentators to have an accurate electronic band structure description when Sb or As are replaced by Te or Ge. More precisely, these substitutions raise the question whether Te and Ge atoms can be located only on either the $12d$ or the $16f$ site or on both sites. It is interesting to notice that a $16f$ site preference of the Ge atoms in the $\text{Re}_3\text{As}_{7-x}\text{Ge}_x$ system has been unambiguously demonstrated from neutron diffraction experiments as a result of the larger difference in the neutron scattering factors (As: +6.58 fm and Ge: +8.19 fm).¹⁹ In the case of the $\text{Mo}_3\text{Sb}_{7-x}\text{Te}_x$ system, the $12d$ site preference of the Te atoms has been only postulated on the basis of electronegativity considerations, but neither experimental nor theoretical evidence have been advanced to ascertain this site preference.¹⁶

The aim of this paper is to show the site preference of Te atoms via electronic band structure calculations in the framework of Korringa-Kohn-Rostoker²⁰⁻²² (KKR) method with Coherent Potential Approximation (CPA) and neutron diffraction study on two $\text{Mo}_3\text{Sb}_{7-x}\text{Te}_x$ compounds with $x = 0$ and $x = 1.6$. We demonstrate that the partial exchange of antimony by tellurium is energetically more favourable on the $12d$ site, results further corroborated by Rietveld refinement on the neutron diffraction patterns. To further corroborate our theoretical statements, similar site energies calculations have been performed on the $\text{Re}_3\text{As}_{7-x}\text{Ge}_x$ system and were found to be in very good agreement with the neutron diffraction study previously reported by Soheilnia et al.¹⁹ suggesting the $16f$ site preference of the Ge atoms. To go

further, plotted DOS of both the Te and Ge atoms on the $12d$ and $16f$ sites have been considered to try to elucidate the origin of such site preferences from an electronic point of view.

II. Experimental and computational details

Synthesis. Phases of nominal composition Mo_3Sb_7 and $\text{Mo}_3\text{Sb}_{5.4}\text{Te}_{1.6}$ were prepared by reaction of stoichiometric amounts of pure Sb powder (5NPlus, 99.999%), Mo powder (Cerac, 99.999%) and Te powder (5NPlus, 99.999%) in sealed evacuated quartz ampoule under He/ H_2 atmosphere. The tubes were then transferred into a programmable furnace and heated up to 750°C for 10 days. At the end of the process, the silica ampoule was quenched in cold water. The solid products were then ground in an agate mortar into a fine powder ($< 100 \mu\text{m}$) and further compacted into pellets in a steel die. To ensure good homogeneity of the samples, these pellets were annealed in a quartz ampoule under He/ H_2 atmosphere at 750°C for 7 days. The final products were powdered again and densified by hot pressing in a graphite dies in an argon atmosphere at 600°C for 2h under 51 MPa. The relative density, defined as the ratio of the measured density to the theoretical density, is 93% and 90% for the Mo_3Sb_7 and $\text{Mo}_3\text{Sb}_{5.4}\text{Te}_{1.6}$ compounds respectively.

Crystal Structure and Chemical Analysis. X-ray powder diffraction (XRD) was performed on the ground materials obtained before the sintering process. Experiment was conducted with a Siemens D500 diffractometer using $\text{CoK}\alpha$ radiation and equipped with a curved primary beam monochromator and a linear detector (PSD). X-ray diffraction pattern was recorded in the θ - 2θ mode between $20^\circ \leq 2\theta \leq 110^\circ$ with a 2θ step of 0.032° and a total counting time of 3h. To obtain accurate lattice parameter, high-purity silicon ($a_0 = 5.4309 \text{ \AA}$) was added as an internal standard. Rietveld refinement against the XRD pattern did not enable

us to differentiate tellurium from antimony. Therefore, to glean more information, we carried out neutron diffraction study.

EPMA analysis confirms the x-ray measurements as it reveals that both the Mo_3Sb_7 and $\text{Mo}_3\text{Sb}_{5.4}\text{Te}_{1.6}$ samples are homogeneous with a very good correlation between the real and nominal composition.

Neutron diffraction. Neutron diffraction data were collected on 3g of Mo_3Sb_7 and $\text{Mo}_3\text{Sb}_{5.4}\text{Te}_{1.6}$ powder on the time-of-flight diffractometer POLARIS at the ISIS facility, Rutherford Appleton Laboratory, U.K. ^3He tube detector banks at 35° , 145° and the ZnS scintillation detector bank at 90° were used. This allows us to access an overall d-spacing spanning the range $0.3 \leq d \leq 8 \text{ \AA}$. Neutron data were acquired for 2h at room temperature. The measurement was made for an integrated proton current at the production target of $200\mu\text{A.h}$. The powder was contained in a vanadium cylindrical can. Rietveld refinement was carried out on the data using the Fullprof program using the 145° bank (backscattering detectors). The relevant crystallographic data from the neutron diffraction analysis are summarized in Table 1.

Electronic Structure Calculations. Electronic structure calculations of the $\text{M}_3\text{X}_{7-x}\text{Y}_x$ ($\text{M} = \text{Mo, Re, X} = \text{Sb, As}$ and $\text{Y} = \text{Te, Ge}$) system ($0 < x < 3$) have been performed by the Korringa-Kohn-Rostoker²⁰⁻²² method with the Coherent Potential Approximation, where the chemical disorder has been treated as a random atom distribution. The description of the alloy including inequivalent sites can be better represented with the chemical formula $\text{M}_3(\text{X1})_3(\text{X2})_4$. In our computations, three types of X-Y disorder have been accounted for: a selective substitution either on the X1 site ($\text{Mo}_3\text{Sb}_{3-y}\text{Te}_y\text{Sb}_4$) or on the X2 site ($\text{Mo}_3\text{Sb}_3\text{Sb}_{4-z}\text{Te}_z$) as well as a random distribution of Y atoms on both X sites ($\text{Mo}_3\text{Sb}_{3-y}\text{Te}_y\text{Sb}_{4-z}\text{Te}_z$). To allow for a direct comparison among computed total energies (E_{tot}) within these three cases, the relation $z = 3/4y$ between the corresponding Te concentrations has been considered. The

self-consistent crystal potential of the muffin-tin form was constructed within the Local Density Approximation (LDA) applying the Barth-Hedin formula for the exchange-correlation part. For well-converged charges and potentials, total, site-decomposed and l-decomposed densities of states (DOS) were computed. Noteworthy, the electronic structure of perfectly ordered compounds, Mo_3Sb_7 and $\text{Mo}_3\text{Sb}_4\text{Te}_3$, have also been considered by the full potential KKR calculations and detailed results are presented in the parallel work dedicated to the thermoelectric properties of some $\text{Mo}_3\text{Sb}_{7-x}\text{Te}_x$ compounds.²³ In this paper, we focus mainly on the electronic structure origin of the site-preference by comparing all contributions to the total energy (E_{tot}), basing our statements on KKR-CPA results as well as from plotted DOS. The lattice constants and positional parameters of Mo (12e) and Sb2 (16f) atoms used for computations were interpolated from the experimental crystallographic data, available for the $x = 0$ and 1.6 samples.

III. Results and discussion

Structural Analysis. The x-ray diffraction pattern of the $\text{Mo}_3\text{Sb}_{5.4}\text{Te}_{1.6}$ compound is shown in Fig. 2. This Te substituted compound crystallizes isotypic with the binary Ir_3Ge_7 structure type (space group $Im\bar{3}m$) and no contributions from secondary phases can be observed. This feature suggests that all the tellurium has reacted and is consistent with previous studies reported on this system.^{16,17} Whatever the sample is, neutron diffraction analysis was performed using the published XRD data on the Mo_3Sb_7 compound as a starting model. Since x-ray and EPMA analysis showed that both materials can be considered as single phase, no secondary phases were added in the model. Rietveld refinement of neutron time-of-flight diffraction pattern is represented in Fig. 3a and Fig. 3b for Mo_3Sb_7 and $\text{Mo}_3\text{Sb}_{5.4}\text{Te}_{1.6}$ respectively. The refinement of the neutron data of Mo_3Sb_7 easily converged to

a fully ordered atom arrangement with regard to the respective site distribution of Mo and Sb atoms and therefore led to good agreement factors (Table 2). The relevant parameters of this structure are listed in the Table 3 and 4. To study the possible site preference of tellurium in the $\text{Mo}_3\text{Sb}_{7-x}\text{Te}_x$ system, three models have been compared with either all the Te atoms located on the $12d$ site (i.e. 53.3% Te and 46.7% Sb), on the $16f$ site (i.e. 40% Te and 60% Sb) or on both sites (i.e. 26.6% Te on the $12d$ site and 20% Te on the $16f$ site). In each case, the structural parameters deduced from the Mo_3Sb_7 compound were used as the starting model. The model dealing with the Te atoms located on the $12d$ site then leads to the best residual factors (Table 5). It should be mentioned that the difference in the three models studied is significant enough to conclude taking into account the similar scattering length of Sb and Te (Sb: +5.57 fm and Te: +5.80 fm). Crystallographic details including atomic positions, isotropic displacement parameters and selected bond lengths are summarized in Table 6 and 7. Because of expected strong correlation between the thermal displacement parameter and the level of occupancy of each site, the site occupancy factor was fixed at the value determined from EPMA analysis and refinement of anisotropic ADP were carried out. It is worth noticing that the presence of Te in the structure results in a slight decrease of the lattice parameter while the opposite trend has been reported for the $\text{Re}_3\text{As}_{7-x}\text{Ge}_x$ compounds.¹⁹ As a conclusion, the neutron diffraction study suggests that Te atoms are only located on the $12d$ site. As we discuss below, band structure calculations seem to reinforce this picture.

Electronic Structure Calculations. The KKR-CPA total energies of disordered systems, where Sb1 ($12d$), Sb2 ($16f$), As1 ($12d$) and As2 ($16f$) were replaced (either preferentially or randomly) by Te and Ge in the $\text{Mo}_3\text{Sb}_{7-x}\text{Te}_x$ (Fig. 4a) and $\text{Re}_3\text{As}_{7-x}\text{Ge}_x$ (Fig.4b), respectively, were calculated as a function of the Te and Ge concentration. In an effort to clearly observe even small variations, the energy difference, ΔE , between a random configuration (Te located on both sites corresponding to E_{rand}) and a selective occupation have

been considered (E_{12d} , E_{16f}). These dependences unambiguously show that the higher the Te and Ge concentrations are, the higher is the energy difference between the two possible sites, the $12d$ site being energetically more favourable in the $\text{Mo}_3\text{Sb}_{7-x}\text{Te}_x$ compounds while the opposite behaviour can be observed in the $\text{Re}_3\text{As}_{7-x}\text{Ge}_x$ system i.e. a $16f$ site preference. Furthermore, these differences are significant enough even for low Te and Ge concentrations (~ 4 mRy for $x = 0.4$ and ~ 2 mRy for $x = 0.4$, respectively) and clearly testifies to the site preference of these atoms. These results are in a very good agreement with the experimental evidence advanced by Soheilnia et al.¹⁹ in the $\text{Re}_3\text{As}_{7-x}\text{Ge}_x$ system and in the present paper for the $\text{Mo}_3\text{Sb}_{7-x}\text{Te}_x$ system.

To try to better understand this behaviour from an electronic point of view, we plotted the DOS contributions of Sb and Te atoms ($\text{Mo}_3\text{Sb}_{7-x}\text{Te}_x$) in Fig. 5a and of As and Ge atoms ($\text{Re}_3\text{As}_{7-x}\text{Ge}_x$ with $x \sim 0.25$) in Fig. 5b for the $16f$ and $12d$ sites. The Sb contribution to the density of states at the Fermi level E_F is substantially higher on the $12d$ site while the Te DOS at E_F is quite small. This is in contrast with the $16f$ site where the Te contribution at E_F has almost the same value while the Sb one is strongly lower. However, the most striking result of these computations is the ‘rigid’ displacement tendency of the entire Te spectrum towards lower energies on the $16f$ site. This could be the main reason of the higher decrease of the total energy when Sb atoms are substituted by Te atoms.

The reason for the $16f$ site preference in $\text{Re}_3\text{As}_{7-x}\text{Ge}_x$ is slightly different. Note that Re_3As_7 is a one-hole metal and that the Fermi level is located above the energy gap. With increasing Ge concentration in $\text{Re}_3\text{As}_{7-x}\text{Ge}_x$, E_F tends to a low DOS energy region. Hence, in the case of As and Ge atoms, the situation is less evident as far as the site preference is concerned. Actually, if we carefully observe the DOS features near the Fermi level, comparable As and Ge DOS contributions can be distinguished. However, one can understand the $16f$ site preference by looking at the sharp DOS peak present just below the energy gap in

both cases (Ge(12*d*) and Ge(16*f*)). Since these peaks strongly contribute to the total energy of the system, it appears to be energetically more beneficial for the $\text{Re}_3\text{As}_{7-x}\text{Ge}_x$ system to introduce Ge atoms on the 16*f* site rather than on the 12*d* site due to the substantially lower DOS peak.

Conclusion

The $\text{Mo}_3\text{Sb}_{7-x}\text{Te}_x$ and $\text{Re}_3\text{As}_{7-x}\text{Ge}_x$ systems have been investigated from band structure calculations using the KKR-CPA method. In both systems, site preferences of the Te and Ge atoms have been clearly demonstrated. While the 12*d* site is energetically more favorable in the $\text{Mo}_3\text{Sb}_{7-x}\text{Te}_x$ system, the $\text{Re}_3\text{As}_{7-x}\text{Ge}_x$ system displays the opposite feature i.e. a 16*f* site preference. These theoretical results are experimentally corroborated by Rietveld refinement on the neutron diffraction patterns of $\text{Mo}_3\text{Sb}_{5.4}\text{Te}_{1.6}$ and $\text{Re}_3\text{As}_6\text{Ge}$ reported in the present study and by Soheilnia et al.¹⁹ respectively.

Acknowledgments

C.C. greatly thanks M. Amiet and P. Maigné, and acknowledges the financial support of the DGA (Délégation Générale pour l'Armement, Ministry of Defense, France) and the Network of Excellence CMA (Complex Metallic Alloys). J.T. acknowledges the support of the Polish Ministry of Science and Higher Education (Grant No. N202-2104-33).

References

- ¹Tritt, T.M. *Science* **1999**, 283, 804-805.
- ²DiSalvo, F.J. *Science* **1999**, 285, 703-706.
- ³Dauscher, A.; Lenoir, B.; Scherrer, H.; Caillat, T. Recent Research Development in Materials Science, Research Signpost, **2002**, 3, 180-207
- ⁴Rowe, D.M. *Thermoelectrics Handbook: Macro to Nano*; CRC Taylor & Francis, 2006.
- ⁵Snyder, G.J.; Toberer, E.S. *Nature Materials*, **2008**, 7, 105-114
- ⁶Ioffe, A.F. *Physics of Semiconductors*; Academic Press: New York, 1960.
- ⁷Slack, G.A. in *CRC Handbook of Thermoelectrics*; CRC Press: Boca Raton, FL, 1995, Section D 34
- ⁸Brown, S. R.; Kauzlarich, S.M.; Gascoin, F.; Snyder, G.J. *Chem. Mater.* **2006**, 18, 1873-1877
- ⁹Brown, S. R.; Toberer, E.S. ; Ikeda, T.; Cox, C.A.; Gascoin, F.; Kauzlarich, S.M.; Snyder, G.J. *Chem. Mater.* **2008**, 20, 3412-3419
- ¹⁰Sales, B.C.; Mandrus, D.; Williams, R.K. *Science* **1996**, 272, 1325-1328
- ¹¹Uher, C. *Semicond. Semimet.* **2001**, 69, 139 and references therein
- ¹²Nolas, G.S.; Cohn, J.L.; Slack, G.A.; Schujman, S.B. *Appl. Phys. Lett.* **1998**, 73, 178-180
- ¹³Candolfi, C.; Lenoir, B.; Dauscher, A.; Bellouard, C.; Hejtmanek, J.; Santava, E.; Tobola, J. *Phys. Rev. Lett.* **2007**, 99, 037006.
- ¹⁴Tran, V.H.; Miiller, W.; Bukowski, Z. *Phys. Rev. Lett.* **2008**, 100, 137004.
- ¹⁵Candolfi, C.; Lenoir, B.; Dauscher, A.; Hejtmanek, J.; Santava, E.; Tobola, J. *Phys. Rev. B* **2008**, 77, 092509
- ¹⁶Dashjav, E.; Szczepienowska, A; Kleinke, H. *J. Mater. Chem.* **2002**, 12, 345-349.
- ¹⁷Gascoin, F.; Rasmussen, J.; Snyder, G.J. *J. Alloys Compd.* **2007**, 427, 324-329.

- ¹⁸Häussermann, U.; Elding-Ponten, M.; Svensson, C.; Lidin, S. *Chem. Eur. J.* **1998**, *4*, 1007-1015.
- ¹⁹Soheilnia, N.; Xu, H.; Zhang, H.; Tritt, T.M.; Swainson, I.; Kleinke, H. *Chem. Mater.* **2007**, *19*, 4063-4068
- ²⁰Korringa, J. *Physica* **1947**, *13*, 392
- ²¹Khon, W.; Rostoker, N.; *Phys. Rev.* **1954**, *94*, 1111
- ²²Bansil, A.; Kaprzyk, S.; Mijnaerends P.E.; Tobola, J. *Phys. Rev. B* **1999**, *60*, 13396
- ²³Candolfi, C. et al. *to be published*

Table 1. Crystallographic data from neutron diffraction experiment on the Mo_3Sb_7 and $\text{Mo}_3\text{Sb}_{5.4}\text{Te}_{1.6}$ compounds.

Chemical formula	Mo_3Sb_7	$\text{Mo}_3\text{Sb}_{5.4}\text{Te}_{1.6}$
fw (g.mol ⁻¹)	1140.1	1149.5
T (K)	298	298
Space group	Im3m	Im3m
Cell dimensions, a(Å)	9.5692	9.5632
V (Å ³)	876.27	874.62
No. formula units per cell	4	4
Calculated density (g.cm ⁻³)	8.64	8.73
T.o.f range (μs)	2000-19000	2000-19000

Table 2. Agreement factors of the Rietveld analysis of the Mo_3Sb_7 pattern.

R_p	0.0278
R_{wp}	0.0217
R_{exp}	0.0130
χ^2	2.78

Table 3. Atomic positions, isotropic and anisotropic displacement parameters (given in Å²) of Mo_3Sb_7 .

Atom	Site	x	y	z	B_{iso} (Å ²)	Occupancy (%)
Mo	12e	0.343(7)	0	0	0.312	100
Sb1	12d	0.25	0	0.5	0.466	100
Sb2	16f	0.162(4)	0.162(4)	0.162(4)	0.456	100

	Mo	Sb1	Sb2
U_{11}	0.00523	0.00388	0.00577
U_{22}	0.00331	0.00691	0.00577
U_{33}	0.00331	0.00691	0.00577
$U_{12}=U_{13}=U_{23}$	0	0	0

Table 4. Selected interatomic distances (Å) of Mo_3Sb_7 .

Mo-Mo	2.990(4) x1
Mo-Sb1	2.821(1) x4
Mo-Sb2	2.800(3) x4
Sb2-Sb2	2.904(2) x1
Sb2-Sb2	3.107(9) x3
Sb1-Sb1	3.383(2) x4
Sb1-Sb2	3.681(7) x8

Table 5. Agreement factors of the three models studied.

	Te located on the 12 <i>d</i> site	Te located on the 16 <i>f</i> site	Te located on both sites
R _p	0.0231	0.0244	0.0240
R _{wp}	0.0182	0.0191	0.0189
R _{exp}	0.0120	0.0120	0.0120
χ ²	2.30	2.53	2.48

Table 6. Atomic positions, isotropic and anisotropic displacement parameters (given in Å²) of the Te substituted Mo₃Sb_{5.4}Te_{1.6} sample (Te atoms located on the 12*d* site).

Atom	Site	x	y	z	B _{iso} (Å ²)	Occupancy (%)
Mo	12e	0.343(7)	0	0	0.256	100
Sb1	12d	0.25	0	0.5	0.408	46.7
Te1	12d	0.25	0	0.5	0.408	53.3
Sb2	16f	0.162(8)	0.162(8)	0.162(8)	0.395	100

	Mo	Sb1-Te1	Sb2
U ₁₁	0.00333	0.00335	0.005
U ₂₂	0.00319	0.00608	0.005
U ₃₃	0.00319	0.00608	0.005
U ₁₂ =U ₁₃ =U ₂₃	0	0	0

Table 7. Selected interatomic distances (Å) of Mo₃Sb_{5.4}Te_{1.6} with all Te atoms located on the 12*d* site (53.3% Te and 46.7 % Sb).

Mo-Mo	2,988(9) x1
Mo-Sb1	2,819(5) x4
Mo-Sb2	2,800(6) x4
Sb2-Sb2	2,886(5) x1
Sb2-Sb2	3,115(1) x3
Sb1-Sb1	3,381(1) x4
Sb1-Sb2	3,676(3) x8

Figure Captions

Figure 1: (a) Antiprisms formed by four Sb1 (in blue) atoms (in blue) and eight Sb2 atoms (in red). The Mo atoms (in green) sit at the centre of each prism. (b) Structural blocks to highlight the empty cube. (c) Unit cell of the binary Mo_3Sb_7 compound.

Figure 2: Rietveld refinement of the x-ray diffraction pattern of $\text{Mo}_3\text{Sb}_{5.4}\text{Te}_{1.6}$.

Figure 3: (a) Neutron diffraction pattern of the Mo_3Sb_7 compound. (b) Neutron diffraction pattern of the $\text{Mo}_3\text{Sb}_{5.4}\text{Te}_{1.6}$ compound.

Figure 4: (a) Sb1 (12*d*) and Sb2 (16*f*) site energies as a function of the Te concentration. (b) As1 (12*d*) and As2 (16*f*) site energies as a function of the Ge content. For sake of clarity, the energy difference between a random configuration and a selective occupation has been considered.

Figure 5: (a) DOS contributions of the Sb (solid black line) and Te atoms (dashed blue line) located on the 12*d* site and 16*f* site. (b) DOS contributions of the As (solid black line) and Ge atoms (dashed blue line) located on the 12*d* and 16*f* site.

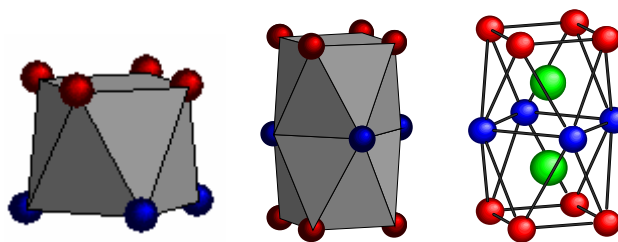


Figure 1a

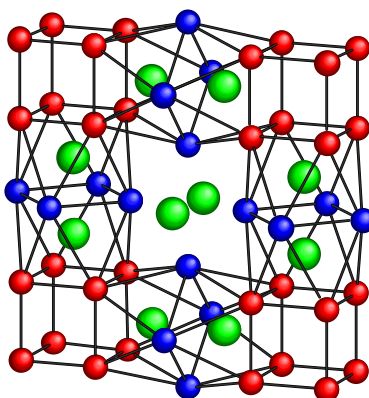


Figure 1b

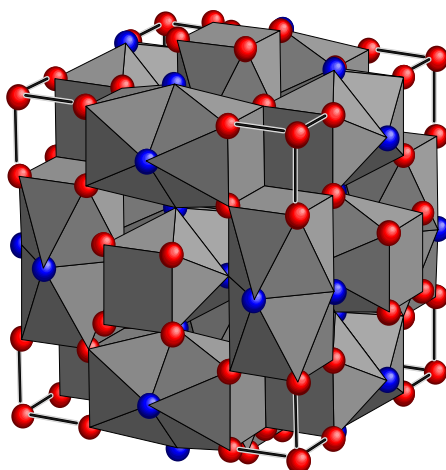


Figure 1c

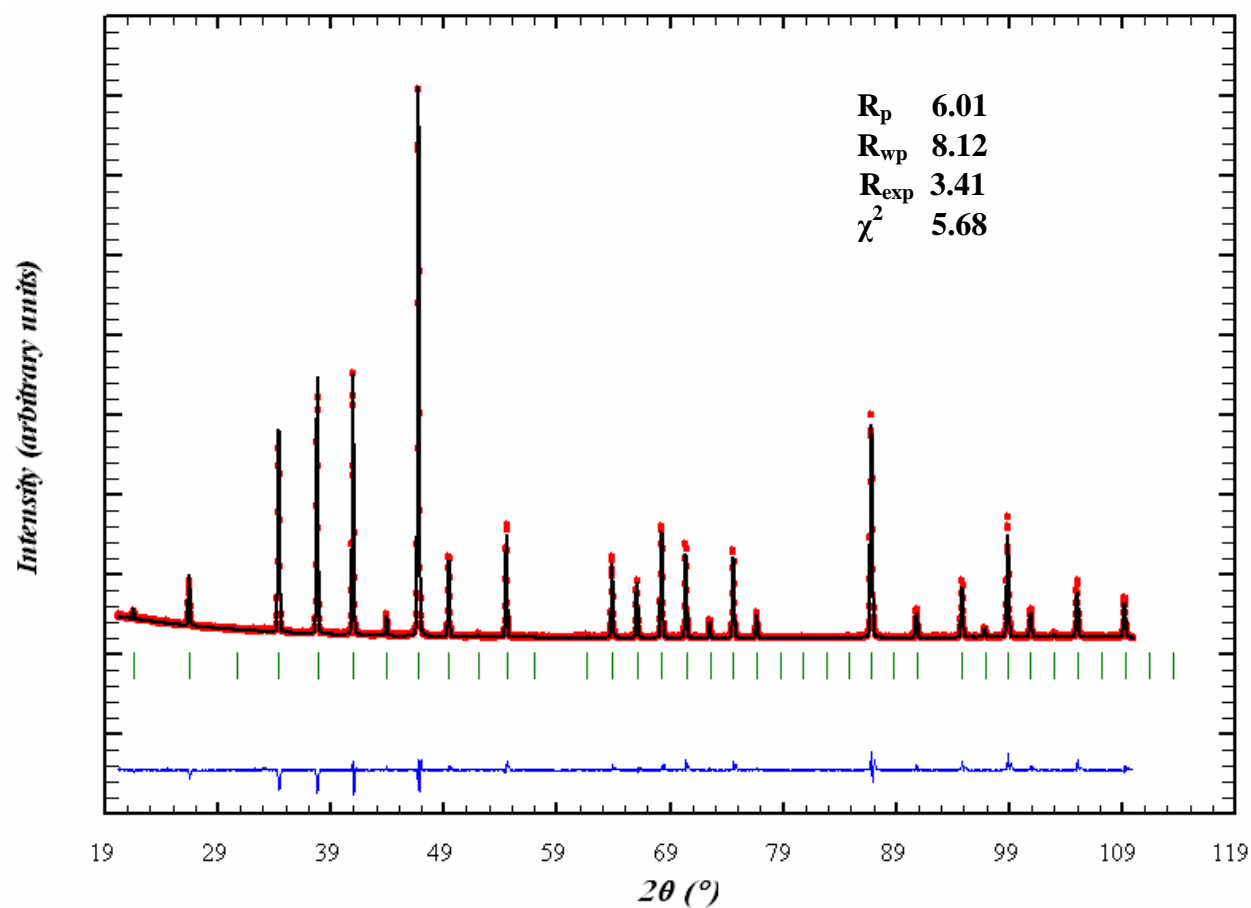


Figure 2

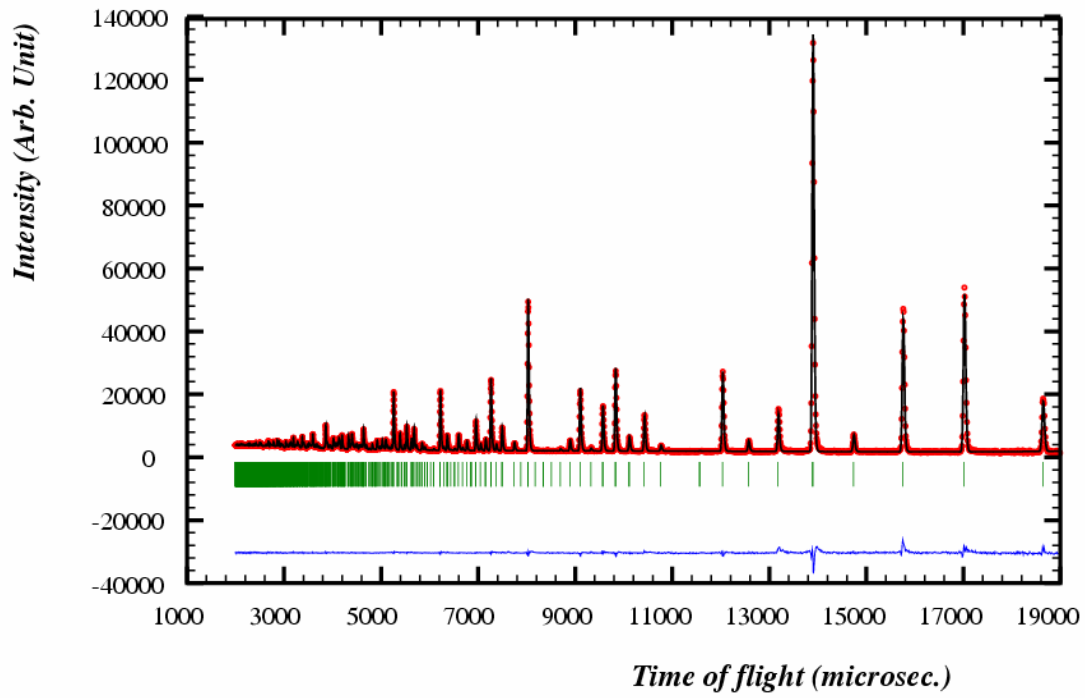


Figure 3a

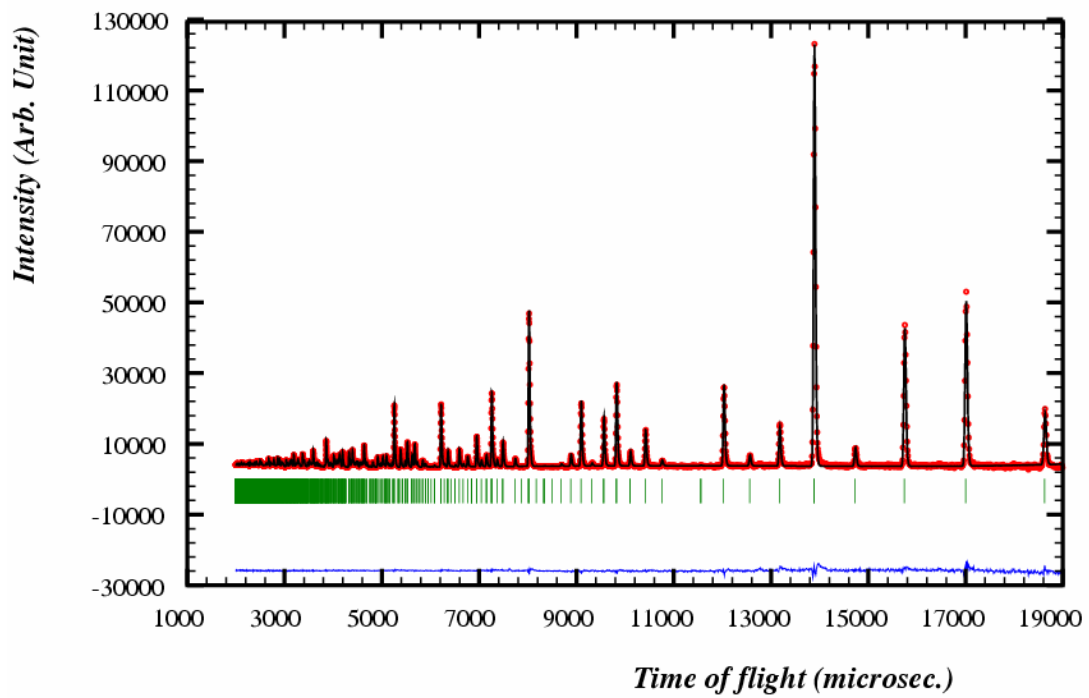


Figure 3b

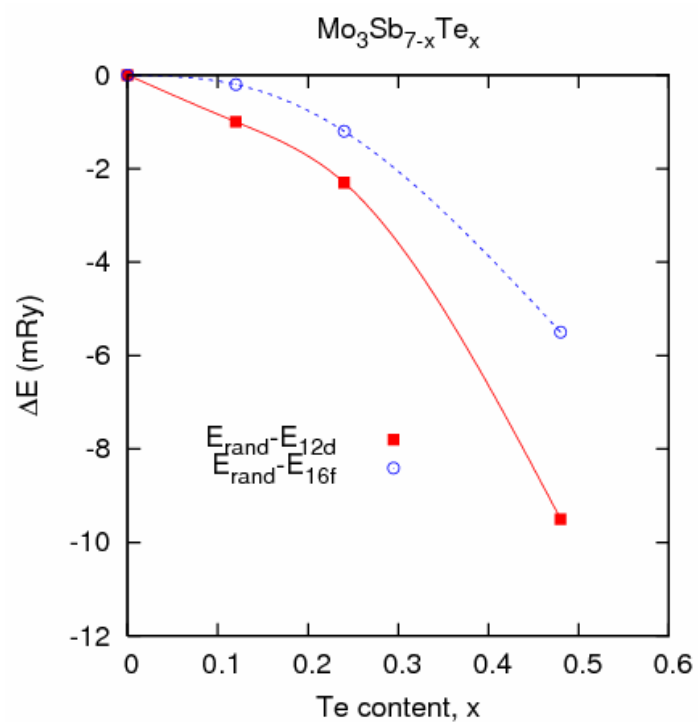


Figure 4a

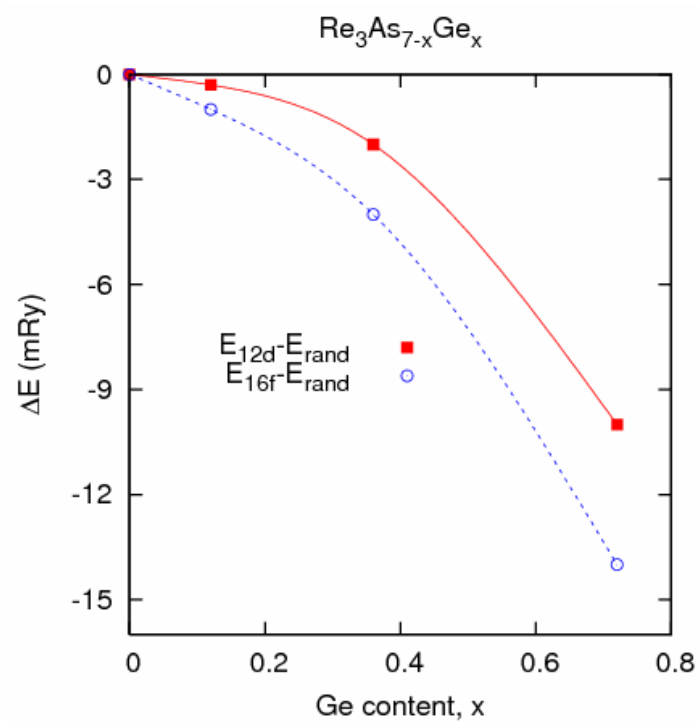


Figure 4b

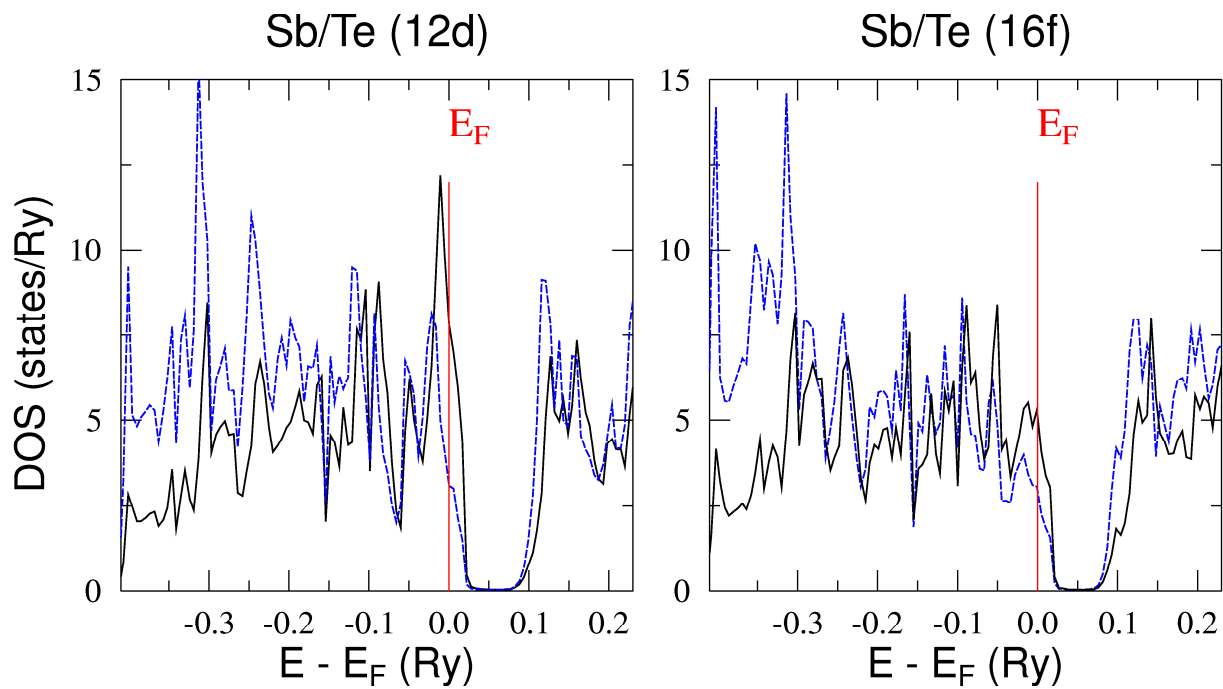


Figure 5a

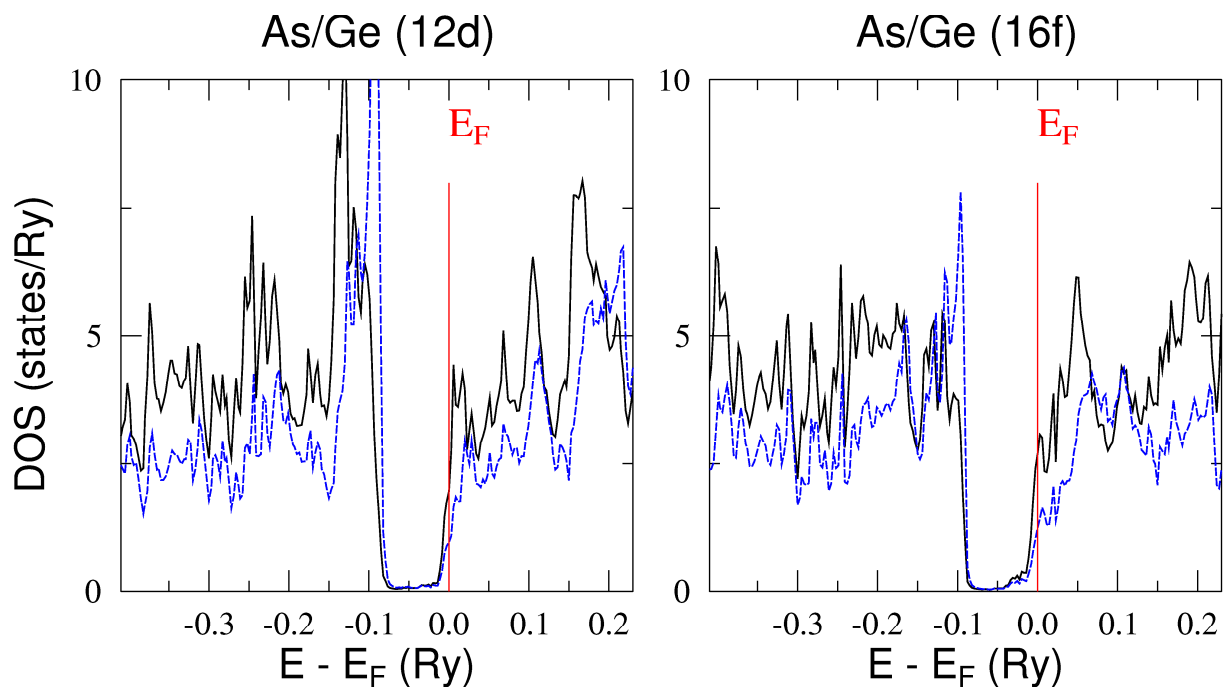


Figure 5b